IEEE Access
Multidisciplinary | Rapid Review | Open Access Journal

Received September 9, 2021, accepted September 29, 2021, date of publication October 8, 2021, date of current version October 19, 2021.

Digital Object Identifier 10.1109/ACCESS.2021.3119213

MPPT Control Paradigms for PMSG-WECS: A Synergistic Control Strategy With Gain-Scheduled Sliding Mode Observer

UMAR HABIB KHAN[1], QUDRAT KHAN[2], LAIQ KHAN[3], WAQAR ALAM[3], NIHAD ALI[4], ILYAS KHAN[5], KOTTAKKARAN SOOPPY NISAR[6], AND RIAZ AHMAD KHAN[7]

[1]Electrical Section, Gomal University, Dera Ismail Khan 29220, Pakistan
[2]Centre of Advanced Studies in Telecommunications (CAST), COMSATS University Islamabad, Islamabad 45550, Pakistan
[3]Department of Electrical and Computer Engineering, COMSATS University Islamabad, Islamabad 45550, Pakistan
[4]Department of Automation, Shanghai Jiao Tong University, Shanghai 200240, China
[5]Department of Mathematics, College of Science Al-Zulfi, Majmaah University, Al-Majmaah 11952, Saudi Arabia
[6]Department of Mathematics, College of Arts and Sciences, Prince Sattam Bin Abdulaziz University, Wadi Al-Dawasir 11991, Saudi Arabia
[7]School of Mechanical and Manufacturing Engineering, National University of Sciences and Technology, Islamabad 24090, Pakistan

Corresponding author: Ilyas Khan (i.said@mu.edu.sa)

ABSTRACT The wind energy conversion system (WECS) frequently operates under highly stochastic and unpredictable wind speed. Thus, the maximum power (MP) extraction, in such unpredictable scenarios, becomes a very appealing control objective. This paper focuses on the extraction of MP from a variable-speed WECSs, which further drive a permanent magnet synchronous generator (PMSG). At the first stage, the dynamical model of the PMSG is converted into Bronwsky form, which is comprised of both visible and internal dynamics. The first-order internal dynamics are proved stable, i.e., the system is minimum phase. The control of the second-order visible dynamics, to track a varying profile of the wind speed, is the main consideration. This job is accomplished via Backstepping-based robust Sliding Mode Control (SMC) strategy. Since, a conventional SMC suffers from inherited chattering issue, thus, the discontinuous control component in SMC scheme is replaced with super-twisting and real-twisting control laws. In addition, the immeasurable states' information are estimated via gain-scheduled sliding mode observer. The overall closed-loop stability is ensured by analysing the quasi-linear form, which supports the separation principle. The theoretical claims are authenticated via simulation results, which are performed in Matlab/Simulink environment. Besides, a comparative analysis is carried out with the standard literature results, which quite obviously outshines the investigated control approaches in terms of varying wind profile tracking and the corresponding control input.

INDEX TERMS Wind energy conversion system, maximum power tracking, sliding mode control strategy, permanent magnet synchronous generator.

I. INTRODUCTION

The increasing demand for electrical energy is the foremost issue across the globe because of the environmental crisis such as the decline in the availability of fossil fuels, emission of greenhouse gases and the various pollution problems. To resolve the issues, the only reliable solution is the consideration of renewable resources, i.e., geothermal, hydro-power, solar, biomass and wind. Relatively, wind energy is the latest form of energy that is cost-friendly and having no undesirable impacts on the surrounding environment [1], [2]. Consequently, the harnessing of wind energy for power generation is an active research area in the last two decades. Researchers believe that investments in the aforementioned area may overtake the market in future.

Commercially available wind turbines are quite capable of conversion but with the addition of minor noise to the outside environment. However, the advanced technologies have resulted in a high quality sophisticated and reliable wind turbines. Generally, the WECS works either autonomously or

The associate editor coordinating the review of this manuscript and approving it for publication was R. K. Saket.

in-grid connected mode. To be more precise, PMSG is more common in power conversion system for the last few years due to its high efficiency, smaller size and reduced cost. Consequently, PMSG-based WECS has been used in wind energy conversion systems. Due to the intermittent and stochastic nature of variable wind speed, the most challenging task in WECS is to extract MP [3], [4]. Particularly, for partial load, the efficiency of WECS is more significant [5]. Therefore, to increase its efficiency, in partial load regime, the maximum power point tracking (MPPT) has been introduced.

Various attempts have been made to compose classical control strategies for WECS, to extract maximum power, but have not been satisfactory due to the uncertain and highly nonlinear dynamical structure of the wind turbine [6]. In model-based control design, the feedback linearization-based control law is convenient but its sensitive nature to the various parametric uncertainties degrades its performance [7]. To address this issue, many nonlinear control schemes are introduced. The smart control techniques such as neural network control strategy [8], Takagi-Sugeno-Kang and Mamdani fuzzy logic control design [9] have been used for WECS. However, these control approaches suffer from long offline training periods and time-consuming computations. Consequently, the sliding mode controller (SMC) can be taken as an alternate option for the WECS owing to its simple design, robustness to parametric variations, insensitivity to an external perturbation. However, the inherited chattering is still an issue that needs to be settled. In the context of robust maximum power extraction from WECS, SMC scheme is proposed in [10], which reduces the adverse effects of the chattering across the switching manifold and improve the total harmonic distortion. Conventional SMC, with super-twisting control law, is proposed in [11], [12] to suppress the chattering phenomena while considering the availability of all the state variables. A feed-forward neural networks-based global SMC is proposed in [13]. The benefits of this method, over [10]–[12], were the uncertain dynamics, which give birth to substantial chattering issues, were estimated via neural networks and the robustness enhancement was claimed. Another very appealing control strategy, combine with terminal SMC approach, was proposed in [14], which resulted in appealing results. It is worthy to mention that state availability is assumed in all the aforesaid SMC strategies, which is somewhat impractical.

In this article, a backstepping-based SMC scheme is synthesized to accurately track the varying wind profile in the WECS. This synergistic control strategy is designed to capture the salient features of both strategies. The nonlinear backstepping-based control strategy allows a step by step procedure to design a stabilizing control law via Lyapunov stability method [15]–[17]. While the SMC scheme alters its configuration according to the system dynamics, thus having the capability to counteract any match disturbances. As discussed in [18], Supper-twisting (ST) and real-twisting (RT) control law suppresses the chattering issue with enough accuracy. Therefore, both supper-twisting (ST) and real-twisting (RT) control laws are used as discontinuous control law instead of conventional signum functions, in the final control structure. This results in the suppressed chattering as compared to feedback linearization and classical SMC. In addition, the newly designed controllers portray robustness against the external disturbances [19]. Since, the final control law needs the states' information, which are unavailable in a practical scenario. Thus, the missing states' information are estimated via a gain-scheduled sliding mode observer. The major contribution includes the synthesis of a Backstepping-based SMC scheme along with a gain-scheduled sliding mode observer. The control law, proposed in this paper, is quite different from [10]–[12] in terms of sliding manifold and the corresponding control structure. In addition, all the system's state variables are reconstructed via a gain-scheduled sliding mode observer, which is not used previously for this particular application in the existing literature. In comparison with the standard literature [7], [13], [14], the proposed techniques have quite an efficient transient response and having zero steady-state error, which is sustained hereafter. Moreover, the corresponding control efforts are also practically feasible.

This paper is organized into the following sections: In section 2, the mathematical modelling of a PMSG is presented. Section 3 describes the input-output form and the investigation of zero-dynamics while the control strategy is developed in section 4. Section 5 and 6 describe the optimal linearized model of PMSG and the formation of gain-scheduled sliding mode observer, respectively. Section 7 covers a wind profiles generation and the simulation results. Finally, section 8 describes the conclusion of the current work.

II. MODELLING OF WIND ENERGY CONVERSION SYSTEM (WECS)

The significant model of WECS includes the aerodynamic model of wind turbine (WT) and model of PMSG, which are connected to an external load.

A. AERODYNAMIC MODEL OF WIND TURBINE

The turbine captures the wind power and converts it into rotational energy. If the turbine rotor captures the wind energy, the actual mechanical power (P_{mech}), available at the PMSG rotor, is quite smaller than the total power due to the stochastic and non-stoppable speed of the wind, which can be expressed as [7]

$$P_{mech} = \frac{1}{2}\rho\pi R_t^2 v_w^3 C_p(\lambda, \beta), \tag{1}$$

where ρ is the density of air, R_t is the radius of WT blade and v_w is the speed of the wind. C_p defines the efficiency of the turbine rotor that is called WT power coefficient. β is assumed to be constant, i.e., ($\beta = 0$), so C_p becomes $C_p(\lambda)$. λ is the ratio between the blade's speed and the wind's speed, which is given as follows

$$\lambda = \frac{R_t \Omega_l}{v_w}, \tag{2}$$

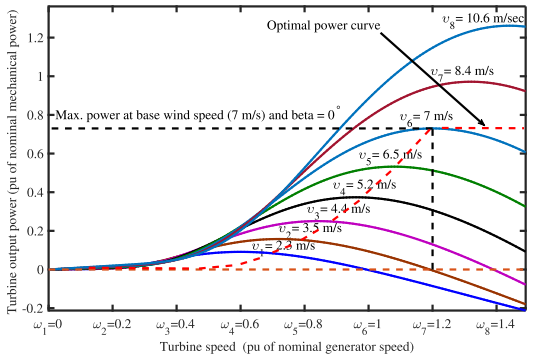

FIGURE 1. Turbine speed vs Turbine output power.

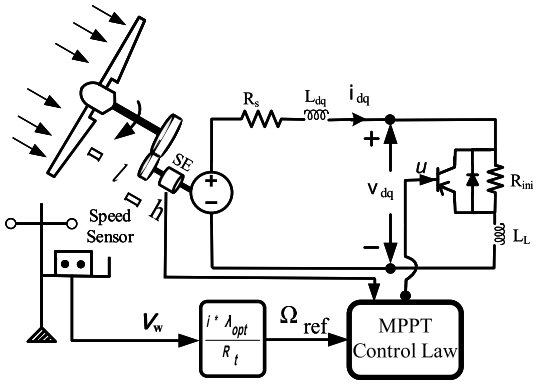

FIGURE 2. Wind energy conversion system based on PMSG.

where Ω_l is the blades rotational speed. Thus, the mechanical output power of WT significantly increases according to the wind speed as clearly seen in Fig. 1. A peak of power is available for every wind speed. These peaks join to form a curve known as optimal regime characteristics (ORC).

For every wind speed v_w, the power coefficient C_p reaches its maximum $C_{p_{\max}}$ whenever λ becomes λ_{opt}. So, to extract the MP from wind, the Tip Speed Ratio (TSR) should operate at its optimal value in such a way that the shaft speed exactly tracks the reference speed, Ω_{ref}, which is calculated from (2), according to the measured speed of the wind, i.e., v_w.

$$\Omega_{ref} = \frac{\lambda_{opt} v_w}{R_t} \tag{3}$$

The power of PMSG rotor can be written as

$$P_{mech} = \Gamma_{wind} \Omega_l \tag{4}$$

According to the wind torque expression, the mechanical torque of the shaft is given as

$$\Gamma_{wind} = 0.5\rho\pi R_t^3 v_w^2 C_T(\lambda), \tag{5}$$

where $C_T(\lambda)$ is the torque coefficient, which can be defined as

$$C_T(\lambda) = \frac{C_p(\lambda)}{\lambda}, \tag{6}$$

where $C_p(\lambda)$, $C_T(\lambda)$ and λ_{opt} are the design parameters, which are usually provided by the wind turbine manufacturer.

B. DYNAMICAL MODEL OF PERMANENT MAGNET SYNCHRONOUS GENERATOR (PMSG)

The dq-model of PMSG, by discarding the zero components, is as follows [20]

$$\left.\begin{aligned} \dot{i}_d &= \frac{-R_s i_d + L_q i_q + v_d}{L_d} \\ \dot{i}_q &= \frac{-R_s i_q - (L_d i_d + \Phi_m) + v_q}{L_q} \\ \dot{\Omega}_h &= \frac{1}{J_h}(\Gamma_{wind} - \Gamma_{em}), \end{aligned}\right\} \tag{7}$$

where v_d and v_q are the dq-axes voltages, R_s is the stator resistance, p is the pole pair number, Φ_m is the permanent magnet flux, Ω_h is the high-speed of the shaft, J_h is the moment of inertia, $\psi_d = L_d\, i_d + \Phi_m$ and $\psi_q = L_q i_q$ are the dq fluxes, respectively. The mathematical expression of electromagnetic torque is $\Gamma_{em} = p\Phi_m i_q$. Furthermore, L_d and L_q are the rotor inductance, which are supposed to be equivalent to each other, i.e., ($L_d = L_q = L$). Thus, we are dealing with a non-salient synchronous generator.

The nonlinear dynamical equations of the PMSG-WECS connected to the load, reported in (7), can be expressed as follows

$$\left.\begin{aligned} \dot{x}_1 &= \frac{-R_s x_1 + p(L_q - L_{ch})x_2 x_3 - R_{ini} x_1}{(L_d + L_{ch})} \\ \dot{x}_2 &= \frac{-R_s x_2 - p(L_d + L_{ch})x_1 x_3 - R_{ini} x_2}{(L_q + L_{ch})} + p\Phi_m x_3 \\ \dot{x}_3 &= \frac{\frac{d_1 v_w^2}{i} + \frac{d_2 v_w x_3}{i^2} + \frac{d_3 x_3^2}{i^3} - p\Phi_m x_2}{J_h}, \end{aligned}\right\} \tag{8}$$

where $[x_1, x_2, x_3] = [i_d, i_q, \Omega_h]$, are the system's states, which represent currents along d-axis, q-axis and the rotational speed of the blades, respectively. In this case, the $\Omega_h = \Omega_l \times i$, with i as the gear ratio. L_{ch} is the equivalent chopper inductance and R_{ini} is the initial value of the chopper equivalent resistance. WECS has a fixed efficiency for the entire speed range, i.e., low speed shaft power, P_l is equal to a high speed shaft power, P_h. The closed-loop structure of WECS is portrayed in Fig. 2.

Remark 1: The dynamical behaviour of electronic components are neglected because of being more rapid than the PMSG dynamics.

In order to operate the system with maximum power, the system in (8) are converted into the control convenient form in the following section.

III. INPUT-OUTPUT FORM

The nonlinear PMSG-WECS model (8) can be expressed in general form as follows

$$\left.\begin{aligned} \dot{x} &= f(x) + g(x)u \\ y &= h(x), \end{aligned}\right\} \tag{9}$$

where $x \in \Re^n$ represent the state vector, $u \in \Re^m$ is the control input, while $f(x)$ and $g(x)$ are nonlinear smooth vector fields which have the following expressions.

$$f(x) = \begin{bmatrix} \dfrac{-R_s x_1 + p(L_q - L_{ch})x_2 x_3}{(L_d + L_{ch})} \\ \dfrac{-R_s x_2 - p(L_d + L_{ch})x_1 x_3}{(L_q + L_{ch})} + p\Phi_m x_3 \\ \dfrac{\frac{d_1 v_w^2}{i} + \frac{d_2 v_w x_3}{i^2} + \frac{d_3 x_3^2}{i^3} - p\Phi_m x_2}{J_h} \end{bmatrix},$$

$$g(x) = \begin{bmatrix} \dfrac{-x_1}{(L_d + L_{ch})} \\ \dfrac{-x_2}{L_q + L_{ch}} \\ 0 \end{bmatrix}$$

where

$$u = R_{ch}$$

The output, $y = h(x) = x_3 = \Omega_h$ is the angular speed of the rotor shaft. Since, our objective is to control Ω_h, therefore, (8) can be transformed into input-output form by defining the following transformation.

$$\left.\begin{aligned} z_1 &= y = h(x) = x_3 = \Omega_h \\ z_2 &= L_f h(x) = \frac{\partial h(x)}{\partial x}.f(x) \\ z_3 &= L_f^2 h(x) = \frac{x_1}{x_2} \end{aligned}\right\} \tag{10}$$

Since the relative degree 'r' of the system ($r = 2$) is one less than the system order n, i.e., ($r < n$) as $n = 3$. So the input-output Bronwsky form appears as follows

$$\left.\begin{aligned} \dot{z}_1 &= z_2 \\ \dot{z}_2 &= L_f^2 h(x) + L_g L_f h(x) u \end{aligned}\right\} \tag{11}$$

$$\dot{z}_3 = -\frac{m_4}{m_1}\left(\frac{k_1 z_3 m_1}{m_4} + \frac{k_2 z_1 m_1}{m_4} + \frac{k_3 z_3 m_1 u}{m_4}\right) + \left(\frac{z_3 m_1}{m_4}\right) \left(\frac{m_4^2}{m_1^2}\right)\left(-\frac{l_1 m_1}{m_4}\frac{l_2 m_1 z_3 z_1}{m_4} - l_3 z_1 + \frac{l_4 m_1 u}{m_4}\right) \tag{12}$$

So, one of the transformed dynamics, i.e., z_3 represents the internal dynamics. The detailed expressions of the Lie-derivatives are given by the following equations.

$$\left.\begin{aligned} L_f^2 h(x) &= -m_4 f_2(x) - (m_2 + 2m_3 x_3) f_3(x) \\ L_g L_f h(x) &= l_4 m_4 x_2 \end{aligned}\right\} \tag{13}$$

Now, it is necessary to discuss the zero-dynamics stability.

A. STABILITY ANALYSIS OF THE ZERO-DYNAMICS

The nonlinear system's dynamics are divided into 2 parts i.e., an internal part and an external (input-output) part when performing the input-output conversion. Since, the external dynamic states, i.e., (z_1, z_2), are controllable states and are directly controlled by u while the stability of the internal dynamic state, i.e., (z_3), is simply determined by the location of zeros called zero-dynamics for a nonlinear system.

To calculate the zero dynamics, the following variables should be set to zero, i.e., $z_1 = z_2 = u = 0$ in (12). By simplifying (12), finally one gets

$$\dot{z}_3 = -z_3(k_1 - l_1), \tag{14}$$

where $k_1 > l_1$, so

$$\dot{z}_3 = -K z_3, \tag{15}$$

where K is a positive integer. So, the zero-dynamic state, z_3 is stable as long as $k_1 > l_1$.

Remark 2: The dynamic model presented in (7) (adopted from [20]) is equivalently represented, in state space form, in (8). The (9) is also the most general form of (8) with vector fields $f(x)$ and $g(x)$ and $u = R_{ch}$ as an affine control input to the system.

IV. BACKSTEPPING-BASED SMC STRATEGIES USING DIFFERENT REACHABILITY LAWS

In this section, the design procedure of Backstepping-based SMC strategy, while using different Reachability Laws, is comprehensively demonstrated.

A. BACKSTEPPING-BASED SMC STRATEGY: USING CONVENTIONAL REACHABILITY LAW (BSMC)

The nonlinear dynamics of the model, given in (11), can be steered to a desired reference by minimising the error between the actual and reference point. Owing to this concept, the error is defined as follows

$$\text{and} \qquad \left.\begin{aligned} e_1 &= z_1 - z_{1ref} \\ e_I &= \int_0^t e_1 \, d\tau \end{aligned}\right\} \tag{16}$$

Now, the design of control law is pursued by defining a Lyapunov function as $V_1 = 1/2{e_1}^2$ and its time derivative along (16) and (11), it becomes

$$\dot{V}_1 = e_1(z_2 - \dot{z}_{1ref}) \tag{17}$$

By selecting z_2 as virtual control law, which is given as follows

$$z_{2ref} = \dot{z}_{1ref} - K_1 e_1 \tag{18}$$

The differential equation (17) is exponential stable, i.e., $\dot{V}_1 = -K_1 e_1^2 = -K_1\, V_1$,, where K_1 is positive constant. To proceed to the next step, we define a new error variable as $e_2 = z_2 - z_{2ref}$. By putting (18), one can obtain $z_2 = e_2 - K_1 e_1 + \dot{z}_{1ref}$, with this (17), which can be expressed as

$$\dot{V}_1 = -K_1 e_1^2 + e_1 e_2 \tag{19}$$

Since, all the error variables are defined. Therefore, a novel sliding surface, in terms of error variables, is defined as follows

$$s = c_1 e_1 + e_2 + c_2 e_I, \tag{20}$$

where c_1 and c_2 are positive parameters. Before proceeding to the control design, it is suitable to make a remark.

Remark 3: It is to be noted that the presented sliding surface is quite novel which is of proportional-integral (PI) type in the conventional error variable e_1 and cumulatively a proportional integral derivative (PID) type surface in the backstepping variable e_2. This kind of sliding surface is not yet used in the existing literature, which makes our design quite novel. The advantage of this surface is that it helps in the elimination of steady-state errors for such stochastic nature desired outputs.

By taking the time derivative of s along (16), and (11), one get the following expression.

$$\dot{s} = c_1\dot{e}_1 + c_2\dot{e}_I + L_f^2 h(x) + L_g L_f h(x).u - \ddot{z}_{1ref} + K_1\dot{e}_1 \quad (21)$$

To calculate the equivalent control law, which drives the system trajectories to an equilibrium point, posing $\dot{s} = 0$ and calculating for the control component, one gets

$$u_{equ} = \frac{1}{L_g L_f h(x)}[-c_1\dot{e}_1 - c_2 e_1 - L_f^2 h(x) - K_1\dot{e}_1 + \ddot{z}_{1ref}] \quad (22)$$

The discontinuous control component is based on the conventional reachability law, therefore, u_{dis} is defined as follows

$$u_{dis} = -K_2(s), \quad (23)$$

where K_2 is the design parameter. Finally, the overall control input, is given as

$$u = u_{equ} + u_{dis} \quad (24)$$

To prove the sliding mode enforcement, a Lyapunov function in terms of the sliding surface is defined as $V = \frac{1}{2}s^2$. The time derivative of this energy function becomes

$$\dot{V} = s\big(c_1\dot{e}_1 + c_2 e_1 + L_f^2 h(x) + L_g L_f h(x)u - \ddot{z}_{1ref} + K_1\dot{e}_1\big) \quad (25)$$

Using u from (24), the above expression reduces to

$$\dot{V} = -K_2|s| \quad (26)$$

This equation can also be written as follows

$$\dot{V} = -K_1\sqrt{(2V)}$$

This equation confirms the finite-time sliding mode enforcement. Consequently, one get the following tracking error dynamics

$$e_2 + c_1 e_1 + c_2\int_0^t e_1 d\tau = 0 \quad (27)$$

This expression shows that $e_1 \to 0$ as $t \to \infty$. As conventional reachability-based law is used, therefore, the control input exhibits chattering issue across the manifold in sliding mode. To get rid of these unwanted effects, it is recommended to use the saturation function instead of the signum function. However, the response may be a bit slower. Thus, in the following study, it is suggested to use the super-twisting law as reachability to alleviate the chattering phenomena.

B. BACKSTEPPING-BASED SMC STRATEGY: USING SUPER-TWISTING REACHABILITY LAW (BSTSMC)

As reported earlier, the objective is to reduce the chattering phenomenon, therefore, the following super-twisting algorithm is used as reachability law.

$$u_{dis} = -\alpha|s|^{\frac{1}{2}}(s) - \beta\int_0^t (s)d\tau \quad (28)$$

Consequently, the overall control law will becomes

$$u_{super} = \frac{1}{L_g L_f h(x)}[-c_1\dot{e}_1 - c_2 e_1 - L_f^2 h(x) - K_1\dot{e}_1 + \ddot{z}_{1ref}] - \alpha|s|^{\frac{1}{2}}(s) - \beta\int_0^t (s)d\tau, \quad (29)$$

where α and β are the constant parameters and s is the sliding manifold based on backstepping variables e_1 and e_2. Note that, the use of super-twisting reachability law does not alter the order of sliding modes, i.e., we are still dealing with first order SMC. However, the benefit gained is the suppression of chattering.

C. BACKSTEPPING-BASED SMC STRATEGY: USING REAL-TWISTING REACHABILITY LAW (BRTSMC)

At this stage, the main interest is to suppress the chattering and to observe the accurate tracking performance. Therefore, a real-twisting-based reachability law is defined as

$$u_{dis} = -\alpha e_1 - \beta e_2 \quad (30)$$

The expression of the controller with this reachability looks as follows

$$u_{real} = \frac{1}{L_g L_f h(x)}[-c_1\dot{e}_1 - c_2 e_1 - L_f^2 h(x) - K_1\dot{e}_1 + \ddot{z}_{1ref}] - \alpha(e_1) - \beta(e_2) \quad (31)$$

It is necessary to mention that the stability analysis from (25)-(27) remains valid for the super-twisting as well as real-twisting sliding mode control law.

Remark 4: In practical implementations, the system (9) may only be available with output. Since, the control algorithm is depending on the output state x_3 as well as x_1 and x_2. Therefore, a state observer is needed to estimate x_1 and x_2. Furthermore, to make simple the stability analysis, one needs to have the separation principle. For this purpose, system (9) in quasi-linear form can be expressed via the following procedure.

V. OPTIMAL LINEARIZATION OF PMSG-WECS

The nonlinear system (9), which is affine in control, at point x_{opt}, can be described as follows

$$\dot{x}_{opt} = f(x_{opt}) + g(x)u = A(x_{opt})x_{opt} + g(x)u \quad (32)$$

At this stage the objective is to get a state-dependable matrix $A(x)$, one may have

$$f(x) = A(x)x \quad (33)$$

or

$$f(x_{opt}) = A(x_{opt})x_{opt} \tag{34}$$

So, following the procedure outlined in [17], assume a_i^T to be the ith row of the matrix $A(x)$. For this purpose (33) and (34) can be rewritten as

$$f_i(x) = a_i^T(x)x, \quad i = 1, 2, \ldots, n \tag{35}$$

and

$$f_i(x_{opt}) = a_i^T(x_{opt})x_{opt} \tag{36}$$

By expanding the left hand side of (35) at x_{opt} and discarding the higher order terms, one gets

$$f_i(x) = f_i(x_{opt}) + \nabla^T f_i(x_{opt})(x - x_{opt}) = a_i^T(x)x, \tag{37}$$

where $\nabla^T f_i(x)\ \varepsilon\ \Re^{n\times 1}$ is the gradient of f_i evaluated at x. Using (36), the above equation can be restated as

$$\nabla^T f_i(x_{opt})(x - x_{opt}) = a_i^T(x_{opt})(x - x_{opt}), \tag{38}$$

In order to get a_i, a constrained minimization problem is expressed as

$$\min_{a_i}\ j = \frac{1}{2}\|\nabla f_i(x_{opt}) - a_i(x_{opt})\|_2^2 \tag{39}$$

The first-order optimally criterion for the augmented cost function $\bar{j}$ is $\bar{j} = \frac{1}{2}\|\nabla f_i(x_{opt}) - a_i(x_{opt})\|_2^2 + \lambda_l(f_i(x_{opt}) - a_i^T(x_{opt})x_{opt})$ with λ_l as Lagrange-Multiplier, results in $\nabla_{ai}\bar{j} = 0$, i.e.,

$$a_i = \nabla f_i(x_{opt}) - \lambda_l x_{opt} \tag{40}$$

The Lagrange-Multiplier, λ_l is determined from (40) with pre-multiplied x_{opt}^T and substituted in (36), the expression of λ_l comes out as follows

$$\lambda_l = \frac{x_{opt}^T \nabla f_i(x_{opt}) - f_i(x_{opt})}{\|x_{opt}\|^2}; \qquad x_{opt} \neq 0 \tag{41}$$

Substitution of (41) into (40) leads to

$$a_i = \nabla f_i(x_{opt}) + \frac{f_i(x_{opt}) - x_{opt}^T \nabla f_i(x_{opt})}{\|x_{opt}\|^2} x_{opt} \tag{42}$$

Using the above formulation, the nonlinear control-focused model of the PMSG-WECS can be expressed as a quasi-linear model of the following form

$$\left.\begin{aligned} \dot{x} &= A_{sys}(x)x + B_{sys}u \\ y &= C_{sys}x, \end{aligned}\right\} \tag{43}$$

where $A_{sys} = [\varphi_{11}, \varphi_{12}, \varphi_{13}; \varphi_{21}, \varphi_{22}, \varphi_{23}; \varphi_{31}, \varphi_{32}, \varphi_{32}]$, $B_{sys} = [-\frac{x_1}{L_d+L_{ch}}, -\frac{x_2}{L_q+L_{ch}}, 0]^T$ and $C_{sys} = \begin{bmatrix}0 & 0 & 1\end{bmatrix}$. Now, the states' estimator, for the above-formulated system is provided in the subsequent section.

Remark 5: Since a quasi linearized model, which supports the separation principles, is obtained for the PMSG-WECS. Therefore, it is quite suitable to design a gain-scheduled robust sliding mode observer for this newly constructed linearized form to provide us with the estimated measurements of the unavailable states of the system.

VI. GAIN-SCHEDULED UTKIN OBSERVER: A SLIDING MODE OBSERVER

The conventional Luenberger observer shows high sensitivity to the disturbance throughout the estimation process. In order to make a robust estimation of the states, an observer based on the concept of the sliding mode is investigated in the following study. The observer, which is presented, has reduced order and it demonstrates a gain-scheduling property that is quite appealing in practical scenarios.

To transform the system into two subsystems, i.e., system with available states and system with non-available states, a similarity transformation of the following form is carried out. Let $T = [N^T \quad C]^T$(where N^T generates the null space of C) be the transformation which transforms (43) to the following form [17]

$$\begin{bmatrix}\dot{z}\\ \dot{y}\end{bmatrix} = TA(x)T^{-1}\begin{bmatrix}z\\ y\end{bmatrix} + TBu \tag{44}$$

and

$$\begin{bmatrix}z\\ y\end{bmatrix} = CT^{-1}x, \tag{45}$$

where $z = [x_1, x_2]^T \in \Re^{2\times 1}$ and $y = [x_3] \in \Re^{1\times 1}$ are unavailable and available information, respectively. The system (44) in more explicit form looks as follows

$$\left.\begin{aligned} \dot{z} &= A_{11}(x)z + A_{12}(x)y + B_1 u \\ \dot{y} &= A_{21}(x)z + A22(x)y + B_2 u \end{aligned}\right\} \tag{46}$$

An observer of the following form is defined to provide the unavailable states.

$$\left.\begin{aligned} \dot{\hat{z}} &= A_{11}(x)\hat{z} + A_{12}(x)\hat{y} + B_1 u + L\upsilon - G_1 e_y \\ \dot{\hat{y}} &= A_{21}(x)\hat{z} + A_{22}(x)\hat{y} + B_2 u - \upsilon - G_2 e_y \end{aligned}\right\} \tag{47}$$

Note that $G_1 \in \Re^{2\times 1}$ and $G_2 \in \Re^{1\times 1}$ represents the gain matrices which improve the performance and show robustness against certain uncertainties. In addition, $L \in \Re^{2\times 1}$ represents the gain of the discontinuous term. υ which is defined as $\upsilon = M_1(\hat{y} - y)$ with M_1 is a real positive constant. The corresponding error dynamics are expressed as follows

$$\left.\begin{aligned} \dot{e}_z &= A_{11}(x)e_z + A_{12}(x)e_y + L\upsilon - G_1 e_y \\ \dot{e}_y &= A_{21}(x)e_z + A_{22}(x)e_y - \upsilon - G_2 e_y, \end{aligned}\right\}, \tag{48}$$

where $e_z = \hat{z} - z$ and $e_y = \hat{y} - y$. Now, to prove further the stability, some new transformation $\varepsilon_z = e_z + Le_y$ are introduced, which leads (48) to the subsequent form.

$$\begin{bmatrix}\dot{\varepsilon}_z\\ \dot{e}_y\end{bmatrix} = \begin{bmatrix}\bar{A}_{11}(x) & \bar{A}_{12}(x)\\ \bar{A}_{21}(x) & \bar{A}_{22}(x)\end{bmatrix}\begin{bmatrix}\varepsilon_z\\ e_y\end{bmatrix} + \begin{bmatrix}0\\ -I\end{bmatrix}\upsilon, \tag{49}$$

with the sub-matrices

$$\begin{aligned} \bar{A}_{11} &= A_{11}(x) + LA_{21}(x), \\ \bar{A}_{12} &= \bar{A}_{21} = A_{12}(x) - \bar{A}_{11}L - G_1 + L(A_{22}(x) - G_2), \\ \bar{A}_{22} &= A_{22}(x) - G_2 - A_{21}(x)L. \end{aligned} \tag{50}$$

The system (49) shows that states observation problem is now appearing as states regulation problem under the action of the discontinuous control υ. To prove that the state converges to zero, the stability analysis is outlined. Consider a Lyapunov function of the following form $V_o = \frac{1}{2}e_y^2$. The time derivative of V_o along (49) becomes

$$\begin{aligned}\dot{V}_o &= e_y(\bar{A}_{21}(x)\varepsilon_z + \bar{A}_{22}e_y - \upsilon),\\ &\leq -\mid e_y \mid (M_1 - |\bar{A}_{21}(x)\varepsilon_z + \bar{A}_{22}e_y|)\\ &\leq -\eta|e_y| \end{aligned} \tag{51}$$

where η is a positive constant and satisfy the following inequality.

$$M_1 - |\bar{A}_{21}(x)\varepsilon_z + \bar{A}_{22}e_y| \geq \eta. \tag{52}$$

The inequality (51), in alternate form, appears as $\dot{V}_o \leq -\sqrt{2}\eta V^{\frac{1}{2}}$ which has the same form as in Lemma 2 of [21]. Thus the error variable e_y converges to origin in a finite-time which is given by

$$t_s \leq \frac{1}{\eta}\sqrt{2V_o(0)}. \tag{53}$$

Note that, the gain L should be selected in such a way that the matrix $\bar{A}_{11} = |A_{11}(x)+L\bar{A}_{21}(x)|$ becomes Hurwitz at each iteration. Similarly, the gain G_2 should be chosen to make $A_{22}(x) - G_2 - A_{21}(x)L = \bar{A}_{22}$ Hurwitz.

It is quite worthy to report that L and G_2 are designed via the conventional linear quadratic regulator (LQR) strategy to place the poles of $\bar{A}_{11}$ and $\bar{A}_{22}$ in the left half-plane (LHP). In the final step, G_1 must be chosen to satisfy $A_{11}(x) = 0$. The suitable selection of these gains, i.e., L_1, G_1 and G_2, will result in infinite time convergence of e_y, where the state $e_z \to 0$ converges asymptotically. Hence, the stability of the observer is proved.

Remark 6: It is necessary to look into the overall closed-loop stability. Since, the system can be expressed in the quasi-linear form, which supports the separation principle. Therefore, in this article, the stability of the controller and observer are performed separately which, in the final stage, proves the overall closed-loop stability, i.e., the stability of the closed-loop plant is subjected to the controller and observer's stability, simultaneously.

VII. SIMULATION RESULTS AND DISCUSSION

In this section, the core objective is to present and discuss the simulation results of the maximum power extraction from the WECS under the action of control algorithms devised in the aforesaid study. The overall study is done by considering two references which mainly vary because of the variations in the system parameters. The closed-loop study, in the presence of controller and observers, is illustrated in Fig. 3.

At this stage, it is convenient to outline the wind profile generation. Since natural wind exhibit irregular variations in wind speed over a long period. It is because of the environmental conditions such as weather, trees, buildings and areas

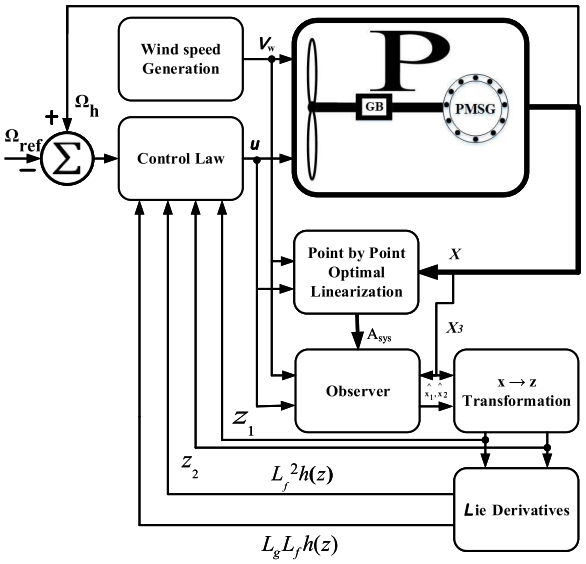

FIGURE 3. The closed-loop block diagram of sensor-less SMC-based PMSG-WECS.

of the sea. Normally, wind speed, which is highly stochastic in nature, can be modelled as follows [7]

$$V(t) = V_s(t) + V_t(t), \tag{54}$$

where $V_s(t)$ is a slowly varying component, which is obtained from the measured data while $V_t(t)$ is a rapidly varying turbulence component. The turbulence component varies, typically within 10 minutes and can be described by power spectrum (von Karman's spectra). The transfer function of the shaping filter is as follows

$$H_t(j\omega) = \frac{K_F}{(1 + j\omega T_F)^{5/6}}, \tag{55}$$

where K_F and T_F depend upon low-frequency wind speed and $V_s(t)$. The non-stationary wind speed can be obtained by the block diagram displayed in Fig. 4. Now, the wind profile-1 is generated by setting the parameters $K_F = 1$ and $T_F = 0.2$ with shaping the filter given in (55). In Matlab/Simulink environment, the simulations are carried out for 3 kW PMSG-based WECS. The numerical solver, used for the simulations, was Euler method with a step size of 0.001 seconds. The other parameters of the system were set as: the maximum power coefficient $C_{p_{\max}} \approx 0.476$, optimal tip speed ratio $\lambda_{opt} \approx 7\ \lambda_{opt}$, the average speed of wind is about 7 m/s and a medium turbulence intensity (using von Karman spectrum) is $\sigma = 0.15$. The closed-loop simulations, according to block diagram reported in Fig. 3, are performed over a period of 50 seconds. Note that all the aforesaid three controllers, i.e., BSMC, BSTSMC and BRTSMC are tested one by one in the closed-loop structure and their comparative results are developed.

Initially, the extraction of maximum power is made possible by operating the turbine at optimum TSR (λ_{opt}) that will ensure $C_{p_{\max}}$ under the action of the designed three control schemes. These optimum values are achieved by controlling

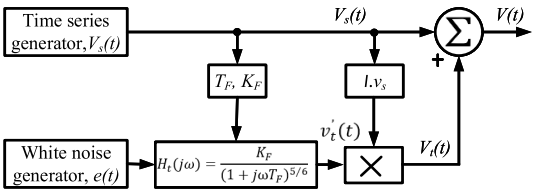

FIGURE 4. Architecture of the non-stationary wind speed generation.

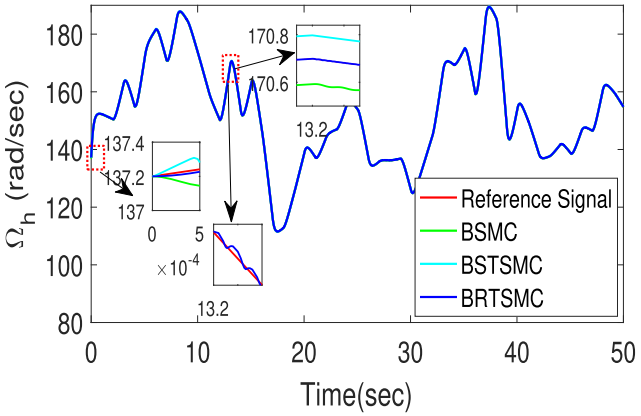

FIGURE 5. Reference tracking via the proposed SMC variants.

the rotational shaft speed of the PMSG. Figs. 5, 6 and 7 ensure the efficient tracking of rotational speed by keeping TSR and power coefficient at its optimum values. Comparatively with the conventional control techniques on the basis of reference tracking, BSMC exhibits high-frequency oscillations as compared to BSTSMC. However, BRTSMC undergoes oscillatory tracking around the reference with comparatively lower amplitude than BSMC and BSTSMC. Furthermore, one can also describes the superiority of the proposed control techniques by observing their settling times, i.e., BRTSMC converges to the desired reference point in 1 second, Which is clearly portrayed in a zoomed section of Fig. 5, whereas, BSTSMC converges to zero in 0.3 seconds while BSMC converges to zero in 1 second. Therefore, it is observed that MPPT is more effective in BRTSMC.

Fig. 5 illustrates the tracking performance of the proposed control strategies with respect to the desired reference. Hence, it is obvious that all the three controllers display very good response with considerably negligible steady steady-state error. On the other hand, the tip speed ratio (TSR) in Fig. 6, the maximum power coefficient in Fig. 7, and the aerodynamic power in Fig. 6 of the BRTSMC controller are quite appealing, as compared to BSMC and BSTSMC. It is quite obvious that the performance of the BRTSMC is comparatively better than BSMC and BSTSMC. However, their performances vary from system to system. It is worthy to note that BSTSMC is easy to implement as compared to BRTSMC because it doesn't require the derivative of the output variable. Since, in the above study, we highlighted that BRTSMC performs better than BSMC and BSTSMC [7]. The comparison

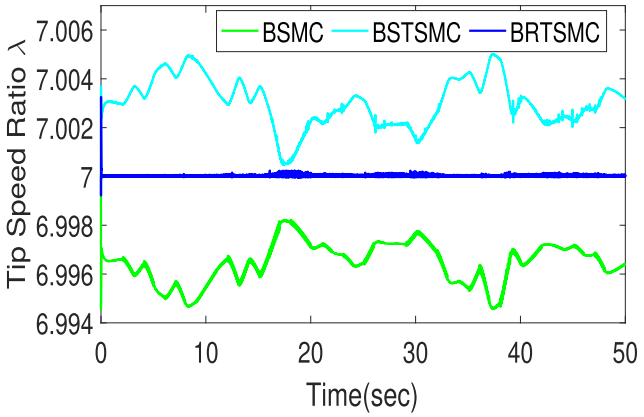

FIGURE 6. Profile of TSR via proposed SMC variants.

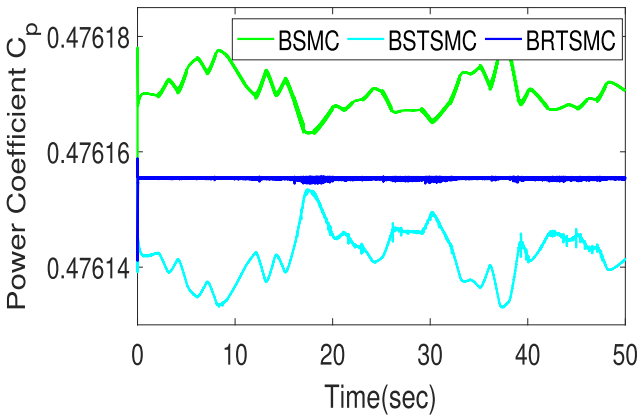

FIGURE 7. Profile of the power coefficient via proposed SMC variants.

is carried out on the basis of tracking performances, TSR, mechanical power coefficient and ORC. It is evident from Fig. 9 that the tracking performance of BRTSMC is better than FBLC. The BRTSMC tracks the reference very closely while that of FBLC exhibits steady-state error, which can be seen in the zoomed picture. Similarly, the other performance parameters are very nicely followed by BRTMC while FBLC lacks in all. See for a detailed look at Figs. 10, Figs. 11 and 12. Thus, it is determined that BRTSMC outshines the other counterparts.

Remark 7: In this work, the performance of the BRTSMC is compared with FBLC. However, if one compares the performance of BSMC and BSTSMC, then it is still confirmed that these two controllers also perform better than FBLC. For the sake of shortness, the detailed presentation is avoided.

To authenticate the performance of the proposed controller, a second wind profile is generated by setting the $K_F = 4$ and $T_F = 10$, while using the same shaping filter $H_t(j\omega)$, which is given (55). Furthermore, to make a simulation platform a bit more practical, it is assumed that the two states, i.e., x_1 and x_2, are not available. So, a virtual sensor, as outlined in the aforementioned theory, is designed via a gain-scheduled sliding mode observer and then the virtually measured states are

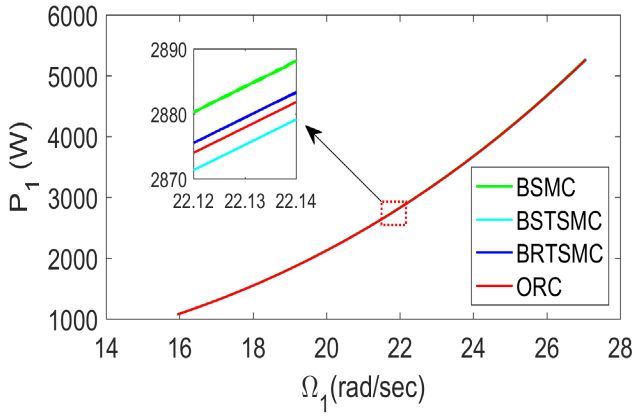

FIGURE 8. Aerodynamics's power profile versus the angular speed of the shaft.

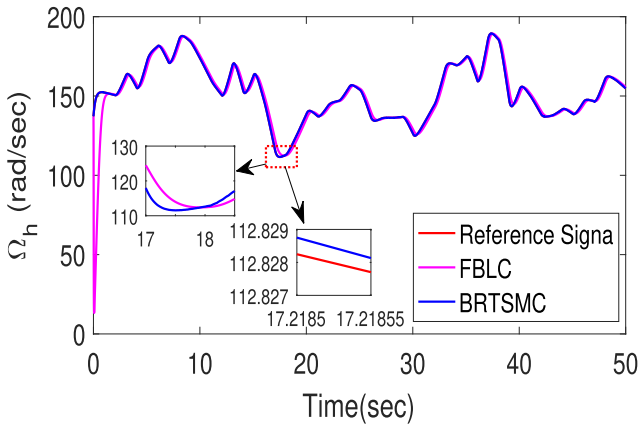

FIGURE 9. Reference tracking via BRTSMC and FBLC [7].

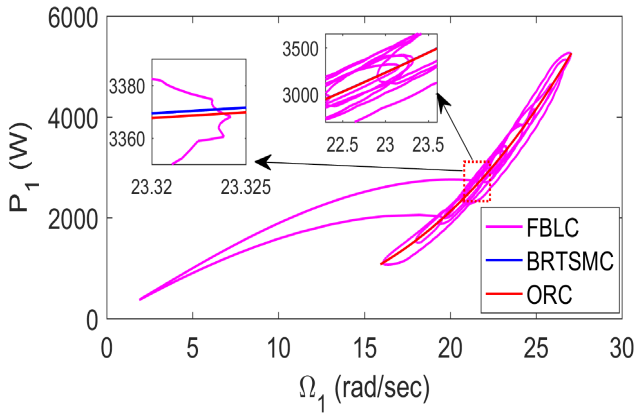

FIGURE 10. Aerodynamic power versus high angular speed in the presence of BRTSMC and FBLC [7].

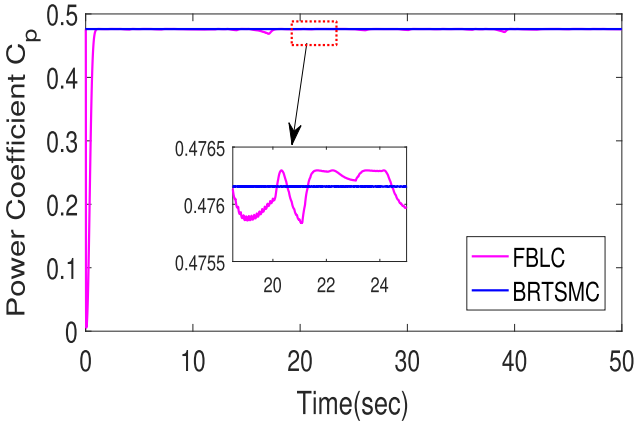

FIGURE 11. Profile of the power coefficient via BRTSMC and FBLC [7].

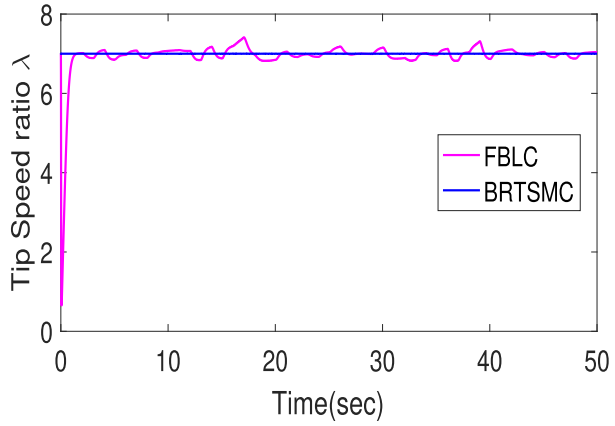

FIGURE 12. Profile of the TSR via BRTSMC and FBLC [7].

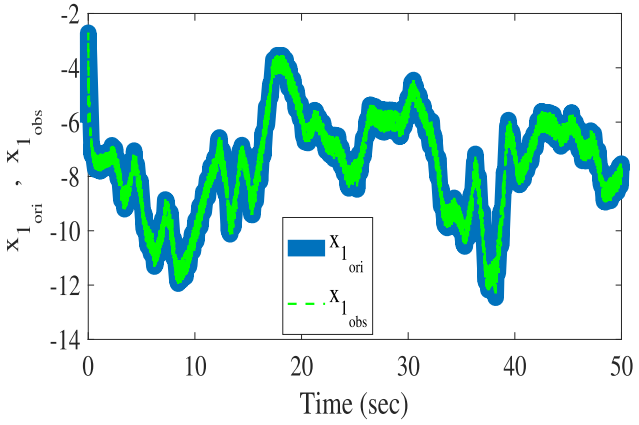

FIGURE 13. Profile of the actual state x_1 and observed state via gain-scheduled SMC observer.

used in the proposed controller. Figs. 13 and 14 show that the missing states are exactly estimated via the gain-scheduled sliding mode observer the so-called gain-scheduled Utkin observer.

Based on the observed states, the simulations are performed and the results are recorded for the proposed control schemes. Fig. 15 illustrates the generated reference speed Ω_{ref} versus the actual speed of the shaft. i.e., Ω_h, where the controller ensures an efficient tracking of the desired trajectory within low span of time. It is pretty obvious that the BRTSMC tracks the reference trajectory with minimum steady-state error (see the zoomed picture) as compared to BSTSMC and BSMC. Fig. 16 shows the profile of wind

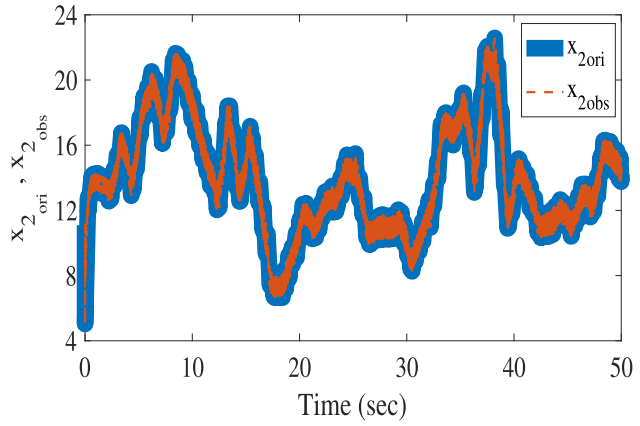

FIGURE 14. Profile of the actual state x_2 and observed state via gain-scheduled SMC observer.

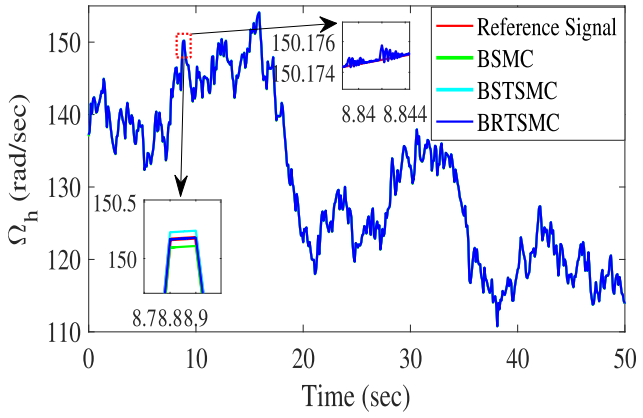

FIGURE 15. Reference tracking of the wind profile, in the presence of the observed states, via proposed SMC variants.

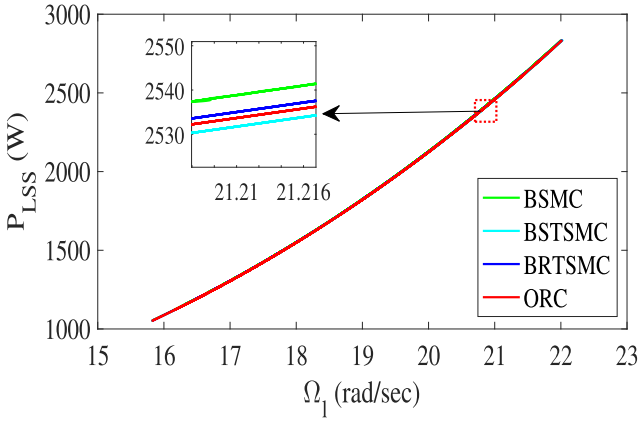

FIGURE 16. Aerodynamic power profile vs the low angular speed of the shaft, in the presence of the observed states, via the proposed SMC variants.

turbine power versus generator actual speed. However, it can be seen that the BRTSMC response lies closer to ORC as compared to BSTSMC as well as BSMC. Similarly, Fig. 17 shows the TSR λ, which is exactly 7, closed to its optimal value in the case of BRTSMC, while the BSTSMC

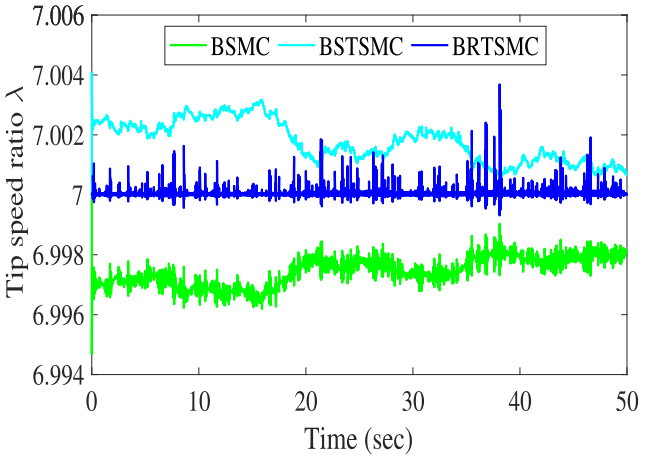

FIGURE 17. TSR, in the presence of the observed states, via the newly proposed SMC variants.

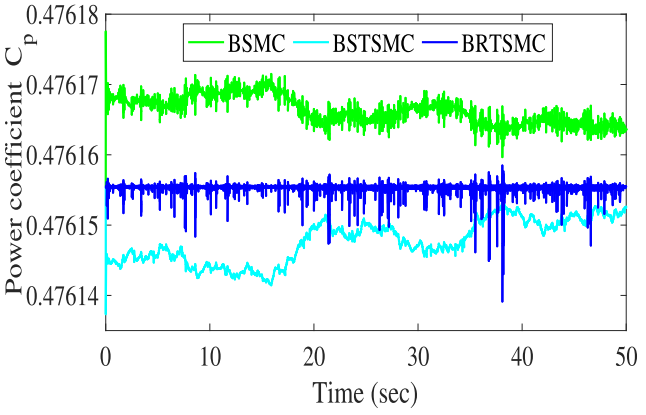

FIGURE 18. Profile of the power coefficient, in the presence of the observed states, via the proposed SMC variants.

and BSMC oscillate around 7. The average wind speed is 7 m/sec.

Finally, Fig. 18 shows the evolution of the power coefficient C_p. It can be seen that the value of C_p is held at $C_{p_{\max}}$ despite all the variations in the wind speed and other parameters. The desirable maximum power coefficient $C_{p_{\max}}$ for the VSWT system is 47% and the BRTSMC lies exactly on 0.47 without oscillations while excursion occurs in BSTSMC and BSMC. Thus, it is confirmed that the newly proposed controllers, based on super-twisting and real-twisting control laws, are appealing candidates for the MPPT-WECS. Its implementation, in other energy applications is highly suggested because of its benefits over FBLC.

VIII. CONCLUSION

In this article, the model-based synergistic control strategies with gain-scheduled sliding mode observers are presented for the tracking of varying wind profile in WECS. The WECS further drives PMSG, which converts wind energy into electrical energy. The core schemes of the synergistic control

laws are Backstepping and SMC approaches, which, when employed in the conventional structure, give us a BSMC strategy. Subsequently, In the aforesaid approach, the discontinuous control law in SMC is replaced by super-twisting and then real-twisting control law, which gives us BSTSMC and BRTSMC, respectively. Since, the designed control strategies, for successful operation, depending on the system's states information. Therefore, a gain-scheduled sliding mode observer (GSSMO) is designed to reconstruct the immeasurable states' information after transforming the nonlinear system into quasi-linear form. The effectiveness of the closed-loop systems, i.e. which include the proposed control strategies and GSSMO, are confirmed via Simulink/MATLAB environment. The results in the presence of load and disturbances were quite appealing and the newly investigated laws proved to be a more practical and appealing candidate for the aforesaid energy system. It is worthy to mention that the simulation results of the proposed strategies are compared with standard literature results. In nutshell, the new strategies especially BRTSMC outshines all the employed designed strategies. The overall closed-loop stability was claimed while taking support of the separation principle.

REFERENCES

[1] D. Song, J. Yang, Y. Liu, M. Su, A. Liu, and Y. H. Joo, "Wind direction prediction for yaw control of wind turbines," *Int. J. Control, Autom. Syst.*, vol. 15, no. 4, pp. 1720–1728, Aug. 2017.
[2] R. Saidur, M. R. Islam, N. A. Rahim, and K. H. Solangi, "A review on global wind energy policy," *Renew. Sustain. Energy Rev.*, vol. 14, no. 7, pp. 1744–1762, Sep. 2010.
[3] M. E. Emna, K. Adel, and M. F. Mimouni, "The wind energy conversion system using PMSG controlled by vector control and SMC strategies," *Int. J. Renew. Energy Res.*, vol. 3, no. 1, pp. 41–50, 2013.
[4] N. Yadaiah and N. Venkata Ramana, "Linearisation of multi-machine power system: Modeling and control—A survey," *Int. J. Electr. Power Energy Syst.*, vol. 29, no. 4, pp. 297–311, May 2007.
[5] R. Fantino, J. Solsona, and C. Busada, "Nonlinear observer-based control for PMSG wind turbine," *Energy*, vol. 113, pp. 248–257, Oct. 2016.
[6] A. D. Martin and J. R. Vazquez, "MPPT algorithms comparison in PV systems: P&O, PI, neuro-fuzzy and backstepping controls," in *roc. IEEE Int. Conf. Ind. Technol. (ICIT)*, Mar. 2015, pp. 2841–2847.
[7] Y. Soufi, S. Kahla, and M. Bechouat, "Feedback linearization control based particle swarm optimization for maximum power point tracking of wind turbine equipped by pmsg connected to the grid," *Int. J. Hydrogen Energy*, vol. 41, no. 45, pp. 20950–20955, 2016.
[8] M. C. Di Piazza and M. Pucci, "Induction-machines-based wind generators with neural maximum power point tracking and minimum losses techniques," *IEEE Trans. Ind. Electron.*, vol. 63, no. 2, pp. 944–955, Feb. 2016.
[9] M. Narayana, G. A. Putrus, M. Jovanovic, P. S. Leung, and S. McDonald, "Generic maximum power point tracking controller for small-scale wind turbines," *Renew. Energy*, vol. 44, pp. 72–79, Aug. 2012.
[10] S. M. Mozayan, M. Saad, H. Vahedi, H. Fortin-Blanchette, and M. Soltani, "Sliding mode control of PMSG wind turbine based on enhanced exponential reaching law," *IEEE Trans. Ind. Electron.*, vol. 63, no. 10, pp. 6148–6159, Oct. 2016.
[11] A. Ullah, L. Khan, Q. Khan, and S. Ahmad, "Variable gain high order sliding mode control approaches for PMSG based variable speed wind energy conversion system," *TURKISH J. Electr. Eng. Comput. Sci.*, vol. 28, no. 5, pp. 2997–3012, Sep. 2020.
[12] G. Zhuo, J. Hostettler, P. Gu, and X. Wang, "Robust sliding mode control of permanent magnet synchronous generator-based wind energy conversion systems," *Sustainability*, vol. 8, no. 12, p. 1265, Dec. 2016.
[13] I. U. Haq, Q. Khan, I. Khan, R. Akmeliawati, K. S. Nisar, and I. Khan, "Maximum power extraction strategy for variable speed wind turbine system via neuro-adaptive generalized global sliding mode controller," *IEEE Access*, vol. 8, pp. 128536–128547, 2020.
[14] M. Zafran, L. Khan, Q. Khan, S. Ullah, I. Sami, and J.-S. Ro, "Finite-time fast dynamic terminal sliding mode maximum power point tracking control paradigm for permanent magnet synchronous generator-based wind energy conversion system," *Appl. Sci.*, vol. 10, no. 18, p. 6361, Sep. 2020.
[15] H. Armghan, I. Ahmad, A. Armghan, S. Khan, and M. Arsalan, "Backstepping based non-linear control for maximum power point tracking in photovoltaic system," *Sol. Energy*, vol. 159, pp. 134–141, Jan. 2018.
[16] S. Rajendran and D. Jena, "Backstepping sliding mode control of a variable speed wind turbine for power optimization," *J. Modern Power Syst. Clean Energy*, vol. 3, no. 3, pp. 402–410, Sep. 2015.
[17] W. Alam, Q. Khan, R. A. Riaz, R. Akmeliawati, I. Khan, and K. S. Nisar, "Gain-scheduled observer-based finite-time control algorithm for an automated closed-loop insulin delivery system," *IEEE Access*, vol. 8, pp. 103088–103099, 2020.
[18] A. Levant, "Higher-order sliding modes, differentiation and output-feedback control," *Int. J. Control*, vol. 76, nos. 9–10, pp. 924–941, Jan. 2003.
[19] N. Schubert and M. J. Schöning, "3. Graduiertentagung der FH Aachen," presented at the 3rd Graduate Symp. FH Aachen-Univ. Appl. Sci., 2010.
[20] I. Munteanu, A. I. Bratcu, N.-A. Cutululis, and E. Ceanga, *Optimal Control of Wind Energy Systems: Towards a Global Approach*. Springer, 2008.
[21] D.-J. Zhao and D.-G. Yang, "Model-free control of quad-rotor vehicle via finite-time convergent extended state observer," *Int. J. Control, Autom. Syst.*, vol. 14, no. 1, pp. 242–254, Feb. 2016.

UMAR HABIB KHAN received the B.Sc. degree in electronics engineering from UET Peshawar, Abbottabad Campus, in 2014, and the M.S. degree in electrical engineering from COMSATS University Islamabad, Abbottabad Campus, in 2019. He is currently an Electrical Supervisor with Gomal University, Dera Ismail Khan. His research interests include robust nonlinear control algorithms, wind turbine systems, solar photo-voltaic (PV) systems, integration of renewable energy sources and control, smart grid, power system stability analysis, and power quality.

QUDRAT KHAN received the B.Sc. degree in mathematics and computer science from the University of Peshawar, in 2003, the M.Sc. and M.Phil. degrees in mathematics from Quaid-i-Azam University, Islamabad, in 2006 and 2008, respectively, and the Ph.D. degree in nonlinear control systems from M. A. Jinnah University, Islamabad, in November 2012.

He was a postgraduate scholarship holder during Ph.D. (2008–2011) and an IRSIP scholarship holder during Ph.D. (as a Visiting Research Scholar at the University of Pavia, Italy). He was selected for the Young Author Support Program, IFAC, World Congress, 2011, Milan, Italy. Since July 2013, he has been working as an Assistant Professor with COMSATS, Islamabad. From September 2015 to August 2016, he worked as a Postdoctoral Fellow with the Department of Mechatronics Engineering, International Islamic University, Malaysia. He has published more than 50 research papers (with an impact factor of 40+) in refereed international journals and conference proceedings. His research interests include robust nonlinear control design, observers design, fault detection in electro-mechanical systems, and multi-agent system's control. He is listed in the Young Productive Scientists of Pakistan in the year 2017 and 2018.

LAIQ KHAN received the B.Sc. degree (Hons.) in electrical engineering from the University of Engineering and Technology Peshawar, Peshawar, Pakistan, in 1996, and the M.S.-leading-to-Ph.D. degree in power system dynamics and control from the University of Strathclyde, Glasgow, U.K., in 2003.

Before his Ph.D. degree, he worked with Siemens Pakistan as a Field Engineer, for a period of two years. He worked as an Assistant Professor with the Faculty of Electronic Engineering, Ghulam Ishaq Khan Institute of Engineering Sciences and Technology, Swabi, Pakistan, in 2008. Then, he joined the Faculty of Electrical Engineering, COMSATS University Islamabad, Abbottabad Campus, Pakistan, and worked as an Associate Professor. He also worked as a Professor at Islamic University Madinah, Saudi Arabia, for a period of three years. He is currently a Professor of power system dynamics and control with COMSATS University Islamabad, Abbottabad Campus. He has published more than 100 papers in highly reputable international conferences and peer-reviewed impact factor journals. His research interests include power system stability and control using PSSs, FACTS controllers and HVDC, robust control theory, intelligent control systems, nonlinear adaptive intelligent control and adaptive predictive intelligent control, fault-tolerant control, power system planning and advanced optimization techniques, nonlinear control of WECS, photo-voltaic systems, micro-grids, and smart-grids.

WAQAR ALAM received the Ph.D. degree in electrical engineering from COMSATS University, Islamabad. He has published several articles in reputed journals. His research interests include nonlinear control theory, adaptive control strategies, and both linear/nonlinear state estimators. In addition, he also serves as a Referee for the Elsevier Research Community.

NIHAD ALI received the B.S. degree in electronic from the University of Engineering and Technology Peshawar, in 2014, and the M.S. degree in control engineering from COMSATS University, Islamabad, Pakistan, in 2017. He is currently pursuing the Ph.D. degree in control science and engineering with the Department of Automation, Shanghai Jiao Tong University, Shanghai, China. His research interests include sliding mode control, adaptive control, and optimal control.

ILYAS KHAN currently works at Majmaah University, Saudi Arabia. He is also a Visiting Professor with the Department of Mathematical Sciences, Faculty of Science, Universiti Teknologi Malaysia, Skudai; UTM Johar Bahru, Malaysia; and the Faculty of Mathematics and Statistics, Ton Duc Thang University, Ho Chi Minh City, Vietnam. He is working on both analytical and numerical techniques. He has published more than 300 articles in various reputed journals. He is also the author of several books and book chapters. His research interests include boundary layer flows, Newtonian and non-Newtonian fluids, heat and mass transfer, renewable energy, and nanofluids.

KOTTAKKARAN SOOPPY NISAR is currently working as an Associate Professor with the Department of Mathematics, College of Arts and Science, Prince Sattam Bin Abdulaziz University, Wadi Al-Dawasir, Saudi Arabia. He has published more than 200 articles and is also a referee of several journals. His research interests include partial differential equations, fractional calculus, and numerical solutions for nonlinear PDEs.

RIAZ AHMAD KHAN received the master's degree in applied mathematics from QAU Islamabad, Pakistan, and the Ph.D. degree in applied mathematics from the National University of Sciences and Technology (NUST), Islamabad, Pakistan. He is currently an Assistant Professor with the Department of Mechanical Engineering, School of Mechanical and Manufacturing Engineering, NUST. His main research interests include nonlinear control systems, mathematical models of infectious diseases, symmetry methods for differential equations, and electrodynamics.